Biomimetic Intelligence and Robotics 3 (2023) 100134

Contents lists available at ScienceDirect

Biomimetic Intelligence and Robotics

journal homepage: www.elsevier.com/locate/birob

Research Article

Aye-aye middle finger kinematic modeling and motion tracking during tap-scanning

Nihar Masurkar [a], Jiming Kang [b], Hamidreza Nemati [a], Ehsan Dehghan-Niri [a,*]

[a] School of Manufacturing Systems and Networks, Ira A. Fulton Schools of Engineering, Arizona State University, Mesa 85212, USA
[b] New Mexico State University, Las Cruces 88003, USA

ARTICLE INFO

Article history:
Received 29 May 2023
Revised 2 November 2023
Accepted 7 November 2023
Available online 14 November 2023

Keywords:
Aye-aye
Kinematics
The lagrangian method
Motion tracking
Tap-scanning

ABSTRACT

The aye-aye (Daubentonia madagascariensis) is a nocturnal lemur native to the island of Madagascar with a unique thin middle finger. Its slender third digit has a remarkably specific adaptation, allowing them to perform tap-scanning to locate small cavities beneath tree bark and extract wood-boring larvae from it. As an exceptional active acoustic actuator, this finger makes an aye-aye's biological system an attractive model for pioneering Nondestructive Evaluation (NDE) methods and robotic systems. Despite the important aspects of the topic in the aye-aye's unique foraging and its potential contribution to the engineering sensory, little is known about the mechanism and dynamics of this unique finger. This paper used a motion-tracking approach for the aye-aye's middle finger using simultaneous video graphic capture. To mimic the motion, a two-link robot arm model is designed to reproduce the trajectory. Kinematics formulations were proposed to derive the motion of the middle finger using the Lagrangian method. In addition, a hardware model was developed to simulate the aye-aye's finger motion. To validate the model, different motion states such as trajectory paths and joint angles, were compared. The simulation results indicate the kinematics of the model were consistent with the actual finger movement. This model is used to understand the aye-aye's unique tap-scanning process for pioneering new tap-testing NDE strategies for various inspection applications.

1. Introduction

Renowned as the largest nocturnal primate in existence [1], the aye-aye exhibits a remarkable tap foraging behavior that sets it apart from other animals. The aye-aye is a strepsirrhine primate native to Madagascar and possesses a distinctive and specialized anatomical feature in the form of a thin middle finger used during their tap foraging [2,3]. The tap foraging process of the aye-aye entails a series of intricate steps. To locate nourishment, it utilizes its elongated third digit to tap on the bark of decaying trees, seeking out cavities that may harbor prey. Once a potential food source is identified, the aye-aye employs its forward-slanting incisors to puncture the wood, creating a small hole. It then proceeds to employ the same narrow middle finger used for taping, skillfully inserting it into the aperture to extract the prized grubs concealed within [4]. The characteristics pertaining to this foraging methodology employed by the aye-aye exhibit similarities to non-destructive evaluation/testing (NDE/T) technologies harnessed by engineers for the evaluation of aging infrastructure, encompassing pipelines, composite materials employed in the aviation sector, and bridges. The aye-ayes have a number of morphological characteristics that distinguish them from other primates, and due to their bizarre feeding ecology and diet, they are considered as an exceptional example of adaptation among mammals [5,6]. They are currently considered one of the world's top 25 most endangered nocturnal lemurs, standing as the sole extant representative of the esteemed Daubentoniidae family [7]. The only living member of the family Daubentoniidae has claws on each digit excluding the thumb [3], an average adult body mass of 2.5 kg [8], a head-body length from 30 to 37 cm and a tail length spanning 74 to 90 cm [9] (refer to Fig. 1). Notably, aye-ayes also have the largest ears relative to head size [10] enhances the aye-aye's acoustic sensing during their tap scanning [11]. Originally, aye-ayes were believed to be insectivorous due to the importance of different insects in their diet [12]. However, the large body size of the animal led some researchers to the argument that they are not strictly insectivorous [13,14]. Actually, they forage upon many food sources with a particular emphasis on larvae. They extract insect larvae from decaying wood on dead or living trees, fallen deadwood, and rarely living trees [13,15]. Consequently, their feeding behavior has become intrinsically associated with foraging within decaying wood. As mentioned, once a cavity is located, they employ their continuously growing incisors meticulously penetrate the exterior of the tree and extract the larvae within using the flexible middle finger [4,16].

* Corresponding author.
E-mail address: nde@asu.edu (E. Dehghan-Niri).

https://doi.org/10.1016/j.birob.2023.100134

Fig. 1. Aye-aye lemurs during tap-scanning (photo: David Haring, Duke Lemur Center).

The acoustic actuation part for the aye-aye is its hand and, more specifically, its slender middle finger. The differences in finger use correspond to significant differences in aye-aye's third and the fourth finger morphology [16,17]. Fig. 2 displays a complete scan of the aye-aye's hand, obtained from the carcass of an aye-aye. The CT was provided by the shared materials instrumentation facility at Duke University. The extraordinary middle digit serves as a probe-like instrument for scanning, locating, and extracting xylophagous (wood-boring) larvae and other types of prey. In general, hand use has been categorized into five distinct classes:

(1) Tapping: The animal taps on a substrate of wooden logs with its third (or occasionally fourth) finger in a stereotypic rhythmic way.
(2) Holding: Aye-ayes are capable of grasping tree bark, branches, or any other objects by forming a grip with multiple fingers. However, it is reported that holding objects in hands is rare in aye-ayes [18].
(3) Probing: After opening an aperture or cavity, the animal probes/inspect any crevice with one of its specialized third or fourth fingers to scrap food or to bring food into [19].
(4) Mouthing: The animal inserts a single finger into its mouth while drinking water or consuming food [20].
(5) Grooming: The aye-aye combs or scratches its fur using one finger of its hand [19].

The morphological attributes of the aye-aye, particularly the distinctive form of its digits and their utilization during foraging, have been the center of several studies. Their hand is proportionately longer than the hand of almost any other primate and exhibits several structural morphologies that are used in locating food. The aye-aye's hand specializations are remarkable, and as mentioned the third digit has evolved with unique capabilities for acoustic actuation in the foraging process. Meanwhile, the remaining digits have retained their original form to help the aye-aye's mobility [17,21]. The aye-aye's third finger serves as a primary instrument for tapping and extracting sustenance from small tree cavities. This finger stands apart from the others due to its relatively slender construction, heightened neuronal density, and enhanced joint flexibility. These exceptional reaching and tapping capabilities result from the metacarpal to which the middle finger is attached. Compared to the fourth finger (the longest), the third finger (the most slender) makes a superior probe for narrow cavities, especially in hardwood trees. However, it should be noted that this delicate finger may be susceptible to significant

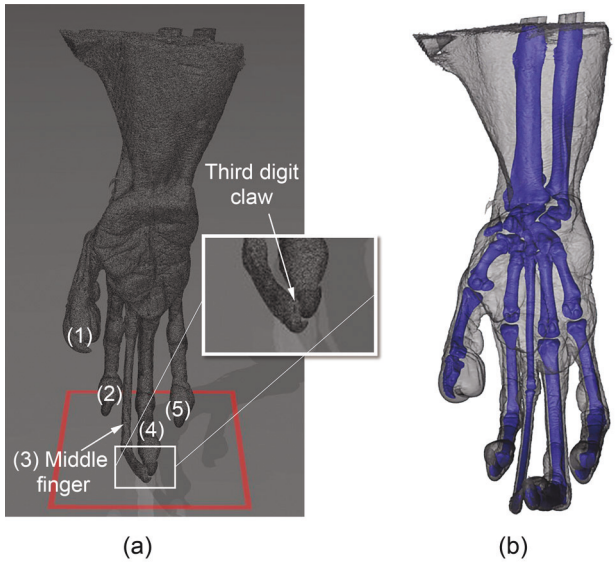

Fig. 2. CT scan of an aye-aye lemur's hand, courtesy of Duke Lemur Center (DLC); (a) a complete scan of the hand with flesh and skin; fingers are numbered consecutively (Enlarged picture shows the third and fourth digits claw) (b) bone structure of the hand highlighted.

bending forces. In contrast, the fourth finger is characterized by its length, sturdiness, robust musculature, and sizeable claw (see Fig. 2). As a result, it is strong enough to play a chief role in securing positional support for the aye-ayes' third finger [16]. Following the tap scanning of a surface by the aye-aye, the resulting variations in sound reflections originating from the diverse interior structures of trees are detected by the animal's large, attentive, and high-frequency-sensitive pinnae. A relatively enlarged inferior colliculus within the aye-aye's brain subsequently processes these acoustic signals. This finger's tapping rate in aye-ayes was estimated at 97.7 ± 19.9 ms, and the dominant energy of each tap was measured between 2 and 27 kHz [5].

Given the aye-aye's distinctive foraging behavior, one may be intrigued by the limited knowledge surrounding its behavioral repertoire. This paucity of understanding primarily stems from the challenges of observing these enigmatic creatures in their natural habitats. The aye-aye's nocturnal lifestyle has impeded researchers from gaining comprehensive insights into its behavioral patterns. Consequently, until relatively recently, the intricate nuances of its behavior remained elusive. In order to surmount this issue, several investigations have been conducted on aye-aye captive aye-aye, affording a closer examination of their developmental milestones and behavioral traits.

Winn described some development behavior of a captive aye-aye during the initial months of its life, providing qualitative and quantitative descriptions of various infant aye-ayes such as vocalizations, locomotion, gaining independence from the mother, as well as defensive and alarm responses [22]. In a separate study, Krakauer et al. examined the hand and body postures of three captive adult aye-ayes. Notably, the aye-ayes exhibited adaptive adjustments in their hand positioning during locomotion, presumably to mitigate the potential stresses exerted on their elongated digits. While traversing oblique and horizontal branches, the researchers observed a greater consistency in body position compared to hand position across all three individuals [23]. Kivell et al. proposed aye-ayes alleviate pressure on their fingers during locomotion by curling their digits away from the substrate. To experimentally investigate this hypothesis, simultaneous video graphics and pressure analysis were employed to assess the hand, foot, and digit movements of five

adult aye-ayes during horizontal locomotion, ascent, and descent on a 30° instrumented runway. The pressure distribution indicated a weight-shifting strategy employed by the animals to reduce loads on their gracile fingers [21]. Furthermore, a study highlighted the unique musculoskeletal morphology of aye-aye's third digit precludes the animal from applying heavy mechanical loads to this finger during locomotion. Consequently, numerous investigations have explored the positioning of this digit as the aye-aye traverses support of varying inclinations. An in-depth review of these similar studies had been previously undertaken by C.E Oxnard, T.L Kivell, and E. Krakauer et al. [21,23,24].

The remarkable foraging behavior of the aye-aye, facilitated by its dexterous fingers, has long attracted attention; however, solid observational data in this regard is still lacking. The manipulation of the aye-aye's fingers has been examined either through direct observation or the analysis of video recordings. Lhota et al. [18] studied hand preference patterns in aye-ayes, comparing their findings with previous studies on captive individuals. They observed that hand preference remained consistent for two of the most frequent behaviors, tapping and probing. Also, it was reported that employing both hands allowed for a wider coverage area during tapping, and enhanced thoroughness during probing into complex cavities. Meanwhile, Feistner et al. conducted observations on free-ranging aye-ayes on an island and reported that tapping occurred within the context of exploration and feeding, predominantly utilizing the elongated third finger. Interestingly, these two behaviors often appeared indistinguishable. Additionally, it was noted that aye-ayes never concurrently employed both hands for specialized finger tasks [25]. Milliken et al. examined and described the frequency of utilization of the third digit during foraging, demonstrating its independent movement from the other fingers [17]. This investigation involved both internal and external video recordings of the apparatus. The third digit's autonomy and multi-axial mobility are facilitated by a unique ball-and-socket metacarpophalangeal joint, endowing the finger with remarkable flexibility [16].

Xu et al. presented an affordable video-tracking system designed for measuring limb motion in small animals. The system employs both intensity-based and color-based algorithms to effectively differentiate the markers and the surrounding background. To enhance accuracy and reliability, an adaptive weighting fusion approach was implemented, enabling the integration of joint positions from multiple trackers. This fusion technique significantly improved the robustness and precision of the tracking system, ensuring more reliable measurement [26]. Weisenberger et al. devised a compact and high-resolution detection and tracking system named single photon emission computed tomography (SPECT) employs infrared (IR) imaging of extrinsic markers to track the animal's movements. The acquired data on the animal's position and orientation were then utilized for motion correction during the process of tomographic image reconstruction. This approach ensured accurate and reliable reconstruction of the mouse's head anatomy in the resulting images [27]. Perner conducted a study on the motion tracking of pigs in stabling, employing an object-oriented method. A reference image was used to discern the object of interest and the background. The masked image was generated using the line-coincidence method. After object correction, the final tracking path and movement parameters were displayed on the screen, providing the operator with valuable information for various purposes [28]. Zhang et al. presented an in-depth investigation into the locomotion mechanism of cheetahs' high-speed movement through the utilization of digital reconstruction techniques. The kinematics and dynamics of the cheetah's leg mechanism were determined by applying the Denavit–Hartenberg (D–H) method [29]. Murray et al. proposed a real-time motion-tracking method with an active camera. The system comprises a movable camera mounted on a pan–tilt platform that intelligently adjusted its viewpoint. Two motion detection techniques, optical flow tracking, and motion energy tracking, were evaluated. The findings demonstrated the system's capability to accurately detect moving edges in dynamic images, enabling effective motion tracking in real-time scenarios [30]. Additionally, Koehnsena et al. presented a motion-tracking methodology utilizing custom JavaScript developed by Adobe Systems and open-source statistical software (R) to track the jumping behavior of locusts. The performance of the tracking system was evaluated by comparing it with simulated videos [31].

While previous studies have primarily concentrated on tracking the overall motion of the aye-aye's hand, little emphasis has been placed on accurately tracking and replicating the intricate motion of its middle finger. In a recent study conducted by the authors [11], a bio-mimetic tap-scanning approach was introduced to imitate the tapping mechanism of the aye-aye. However, it should be noted that the study fell short in fully mimicking the complex dynamics and motion of the middle finger during the tapping process.

The primary contribution of this paper lies in the development of a motion-tracking approach and a hardware model with a two revolute joint configuration (*RR*), both designed to systematically mimic the intricate motion of the aye-aye's middle finger. To achieve this, the study employed a motion-tracking technique to analyze the movement of the aye-aye's middle finger. By capturing video graphics simultaneously, the motion was accurately recorded and analyzed. To replicate this motion, a two-link robot arm model was constructed, allowing for the reproduction of the finger's trajectory. The kinematics of the middle finger was derived using the Lagrangian method, resulting in a comprehensive model that simulated the aye-aye's finger motion. To ensure the accuracy of the model, various aspects of motion, including trajectory paths and joint angles, were compared and validated with a hardware model. The paper is organized into the following sections: Motion Tracking section, which explores the precise measurement and analysis of angular motion and trajectory tracking. The subsequent section, Kinematic Model, focuses on the development of a comprehensive model to describe the intricate motion of the aye-aye's middle finger, along with the utilization of mathematical formulation to ascertain its precise movement. Section 4 presents a comparative analysis between the simulated results and the implementation on hardware. Lastly, the Conclusions section concisely summarizes the valuable findings and profound insights derived from this study.

2. Motion tracking

The experimental methodology presented in this paper is based on a markerless motion tracking approach using the video acquisition software-Kinovea [32]. Puig-Divi et al. demonstrate that Kinovea is a reliable, precise, and valid tool for obtaining angle and distance data from coordinates [33]. The program exhibits both inter-rater and intra-rater reliability, establishing its credibility. The study shows that reliable results can be obtained from perspectives ranging from 90° to 45°, with an orthogonal perspective of 90° being recommended for optimal outcomes. Additionally, Shishov et al. study showcased the successful application of Kinovea in capturing whole-body kinematics from real-life videos [34]. The software effectively tracked joint motions in a 30 Hz video, calculating joint trajectories with a maximum error of 9%. It accurately determined angular positions and velocities within a 13% error range, while peak vertical and horizontal velocities were determined with a 2% error range.

The video footage used in this study was obtained from the National Geographic website, and the frames were captured from the video. The full-length video can be accessed at the following link: https://www.youtube.com/watch?v=Fw2DtZYJuiI. This

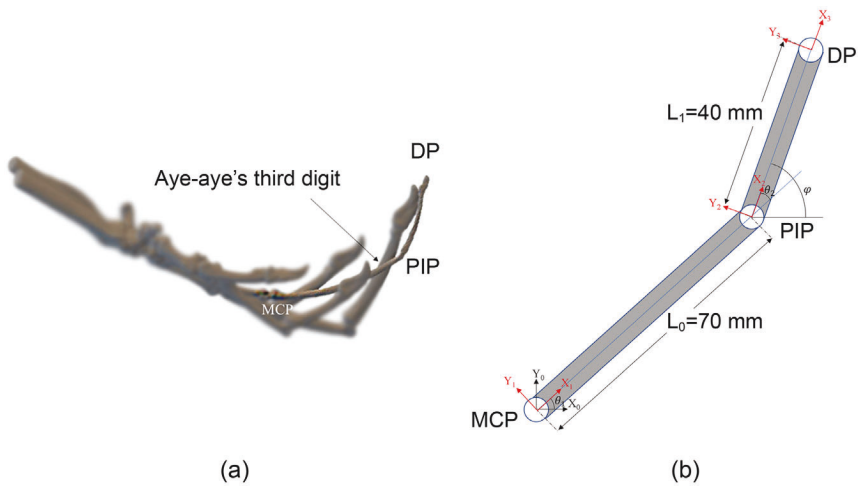

Fig. 3. Aye-aye's middle finger; (a) bone structure of the hand, courtesy of Duke Lemur Center (DLC) (b) description of the third digit as a *RR* robot; Simulink model designed based on the MCP, PIP, and DP joint marker locations on the finger.

video was further processed with the help of Kinovea Motion Tracking Software to track the movement of individual joints.

Aligning with this study's objectives, this paper's primary focus is to detect and analyze the movement focused on the aye-aye middle finger. Miniature markers are chosen at the points of the Metacarpophalangeal Joint (MCP), Proximal interphalangeal Joint (PIP), and Distal interphalangeal Joint (DP) to track the motion of these different joints [35]. As shown in Fig. 3, based on the CT scan of aye-aye's hand provided by Duke Lemur Center (DLC), the distance between the MCP and PIP is 70 mm, and the length from PIP to DP is 40 mm. To understand the motion path of the entire finger, the flexion portions of the angular profiles for the PIP joint are not considered for simplification which will be further verified by the tracking the motion using Kinovea. In other words, the angular change would be exclusively measured in the X-Y plane. As documented by Ramsier and Dominy [5], the precise tapping frequency of the aye-aye is known to exhibit variability, typically falling within the approximate range of 8 to 10 Hz. For the purpose of this study and to enable meaningful comparisons, a "cycle" was defined as the temporal interval separating two consecutive tapping events, specifically when the aye-aye's third digit makes contact with the wooden surface.

2.1. Angular tracking

In order to study the intricate angular motion of the middle finger, the motion paths of the PIP and DP Joints were plotted as visually depicted in Fig. 4. The evolutionary patterns of the joint angles during distinct phases were meticulously examined and observed. When the fingertip DP gets lifted from a touching point (Fig. 4(a)) to a clicking point (Fig. 4(c)), the relative angle decreases from 50.7° to 23.9° because the joint gets relaxed and there is no force or torque on the joint; Subsequently, as the fingertip ascends to a higher position in the air, the joint angle progressively increases to a peak value of 65.4° demonstrating the active stretching of the joint caused by muscular exertion. Shortly thereafter, the angle slightly reduces to 53.9° as the fingertip rapidly approaches the target object at high speed. To gain further insight into the angular dynamics, refer to Fig. 5, wherein the variation in joint angle over time is presented. As seen, the curves are plotted through interpolation using the limited dataset points derived from the finger trajectory calculated on each video frame. For better representation, each subplot has been divided into four segments in a cycle, denoted by quarter 1 (Q_1) to quarter 4 (Q_4). Fig. 5(a), illustrates that the angle(θ_1) of the MCP joint exhibits a similar pattern to that of the PIP joint angle but with a relatively smaller scale. Notably, both angles reach their maximum value at around the same time instances (regions Q_3 and Q_4).

As for the angular velocity, $\dot{\theta}_1$ and $\dot{\phi}$ also share the same pattern (like the trigonometric function cosine). Still, the overall shape is different from the angular (like trigonometric function sine) in Fig. 5(a) since the latter represents the derivative of angular displacement with respect to time. In contrast, the acceleration characteristics are encapsulated in Fig. 5(c). Remarkably, a linear decrease in acceleration is evident for $\ddot{\theta}_1$, attributable to the sole influence of the MCP joint. The MCP joint can be regarded as an actuator propelled by a consistent acceleration, thus elucidating the observed linear decline.

2.2. Path tracking

Similarly, the PIP and DP joint trajectory was tracked during the aye-aye's tapping motion, as seen in Fig. 6. The maximum displacement of the DP joint is 39.83 mm in Fig. 6(e) when the finger stops at the peak of the lifting position, then moves back to 4.63 mm (almost close to the starting point) when the fingertip DP touches the subject. This observation elucidates the repetitive nature of the aye-aye's finger path during tapping, forming a closed-loop trajectory precisely at the designated location. From Fig. 6(e) to Fig. 6(f), one can see there is an acceleration period that enables the fingertip DP to get a maximum velocity of 0.22 m/s, which is helpful to attain its maximum momentum just before contact. Moreover, the path sequence indicates the joint PIP is moving backward first, as seen in Fig. 6(a) to Fig. 6(c), followed by an upward trajectory as illustrated in Fig. 6(e). Notably, the path is not a perfect circle because the origin of the base frame in joint MCP is not fixed, which is a little different from the traditional two-link *RR* robot arm. However, by making slight compensations to the base frame's origin, this new origin of the two-link *RR* robot arm can be regarded as a fixed reference point. Thus, for simulation purposes, a two-link *RR* robot can be considered as a direct replica of the aye-aye's finger.

Furthermore, from the video, the difference between the aye-aye's DP and PIP joints can be plotted with respect to the distance traveled, velocity, and acceleration, as seen in Fig. 7. Similar to Fig. 5, the plots are generated using a limited number of data points for one cycle. Based on the velocity variation plot of DP and PIP joints as seen in Fig. 7(b), it was found that the speed of the DP joint decreases at the outset of the cycle, indicating the fingertip

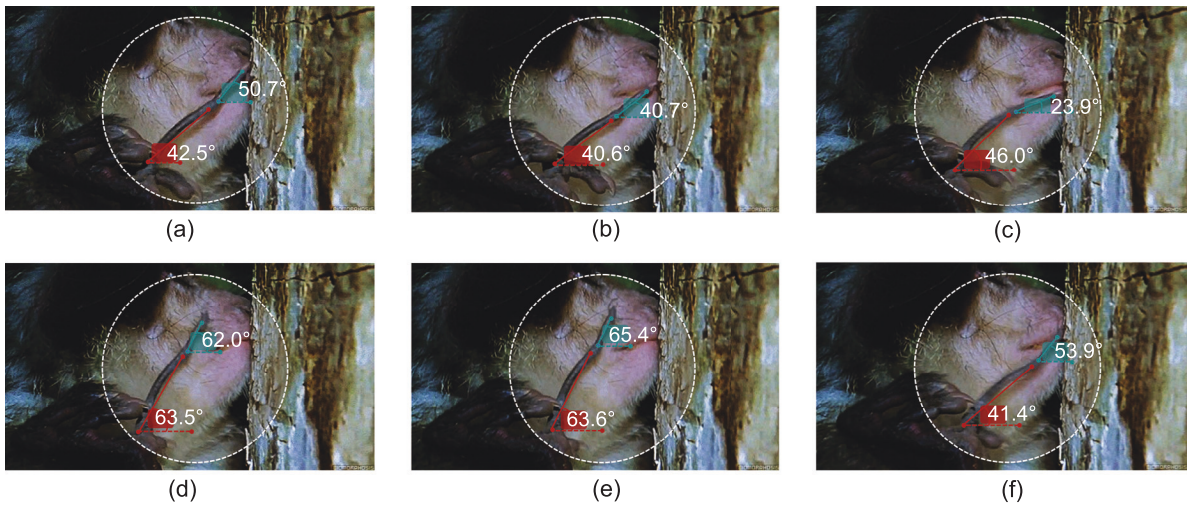

Fig. 4. Kinovea markerless motion tracking results showing the relative path of the aye-aye's finger while tapping.

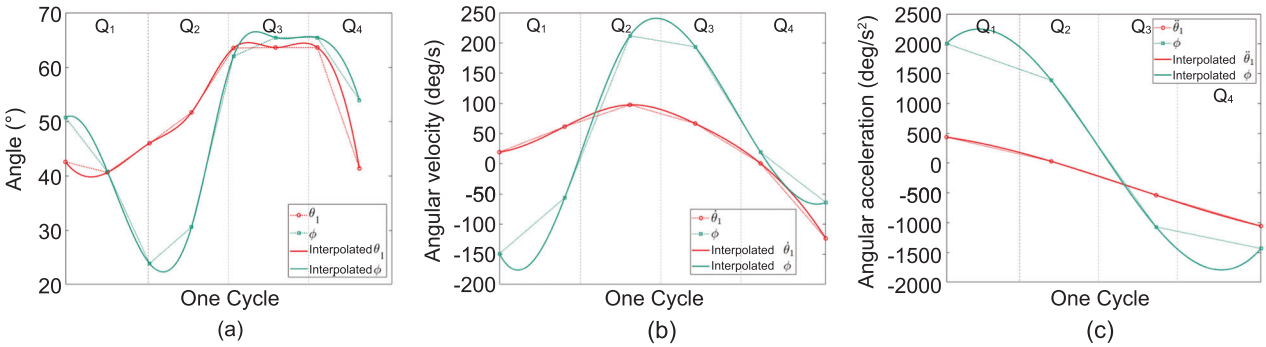

Fig. 5. Kinovea motion tracking results of the angular variation plots of PIP and DP Joints (a) relative angle (b) angular velocity (c) angular acceleration.

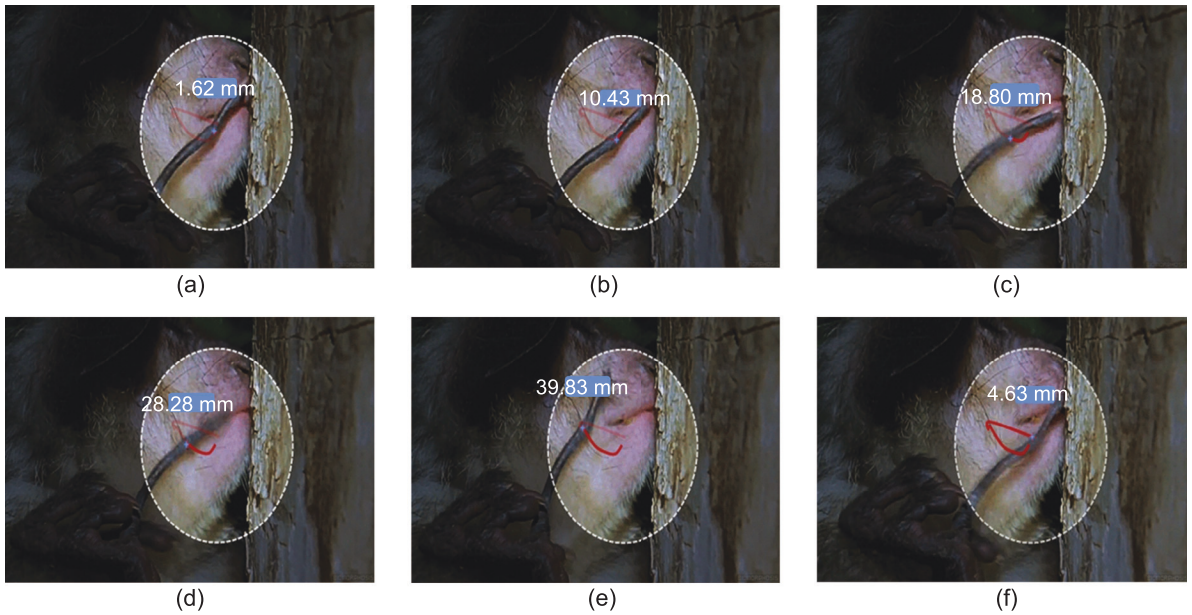

Fig. 6. Kinovea markerless motion tracking results showing the relative path of the aye-aye's finger while tapping.

gets off from the touching point and then gets slightly accelerated and reaches its maximum 0.23 m/s during the second quarter of its cycle, which can be referenced from Fig. 7(c). Subsequently, the speed drops to around 0 m/s at the end of Q_3, which means it reaches the highest point and hangs in the air for a short period of time during transition from Q_3 to Q_4. This condition can be observed in the distance curve Fig. 7(a), which exhibits a gradual and minimal change in distance during this time interval, with

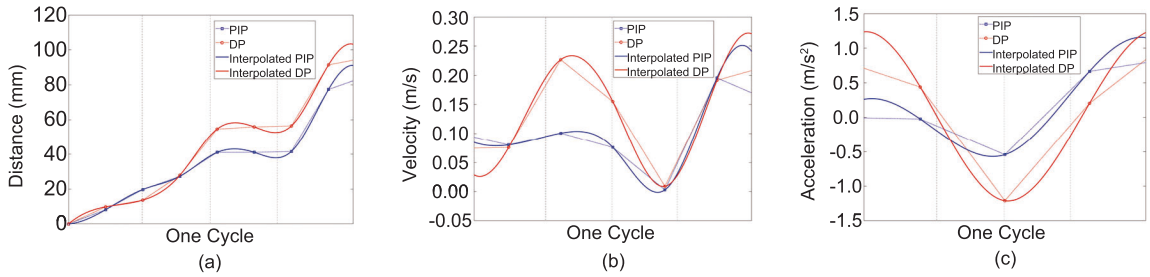

Fig. 7. Kinovea motion tracking results of the speed variation of the middle finger joint DP and PIP (a) distance (b) velocity (c) acceleration.

Table 1
Denavit–Hartenberg parameters of the third finger modeled as two-link arm.

i	α_{i-1}	a_{i-1}	d_i	θ_i
1	0	0	0	θ_1
2	0	L_0	0	θ_2
3	0	L_1	0	0

both curves maintaining a near-horizontal trajectory during the third to the beginning of the fourth quarter in one cycle. Following this period, the fingertip undergoes acceleration, leading to a gradual increase in speed from 0 m/s to its maximum of 0.22 m/s just before making contact with the object.

3. Kinematic model

This section focuses on developing a comprehensive mathematical model to accurately describe the intricate movements of the aye-aye's middle finger. Through a detailed analysis of joint angles, trajectories, and motion parameters, the kinematic model provides a robust framework for understanding and simulating the complex motion dynamics exhibited by the aye-aye's finger.

3.1. Kinematic model development

A simplified mechanical model is developed based on its kinematics to gain insight into the unique mechanical characteristics of the aye-aye's middle finger. When an aye-aye strikes its finger against a wood, its finger joints undergo rotational motion, causing the fingertip to intersect with the target surface at a specific angle. In order to analyze this mechanism, a simplified model is constructed with the following assumptions: (i) the fingertip is straight and rotates about its individual joints; (ii) during tapping, the palm remains fixed; (iii) the finger is described as a two-link revolute jointed (*RR*) robot model (see Fig. 3(b)) ; (iv) the tip of the finger is assumed to be a part of the DP joint thereby assuming it to be a fixed joint.

Table 1 provides the geometric parameters of the robot according to the Denavit–Hartenberg convention [36]. Within this table, i corresponds to the joint number, a_{i-1} denotes the distance along the X_i axis, α_{i-1} refers to the angle between the axes Z_{i-1} and Z_i, d_i represents the distance between the axes and finally θ_i represents angle between the axis X_{i-1} and X_i.

The position and orientation of the fingertip could be obtained through the forward kinematics. It is necessary to calculate the homogeneous transformation matrix T_i^{i-1} of each finger joint using the equation below:

$$T_i^{i-1} = \begin{bmatrix} cos\theta_i & -sin\theta_i & 0 & a_{i-1} \\ cos\alpha_{i-1} * sin\theta_i & cos\alpha_{i-1} * cos\theta_i & -sin\alpha_{i-1} & -d_i * sin\alpha_{i-1} \\ sin\alpha_{i-1} * sin\theta_i & cos\alpha_{i-1} * sin\theta_i & cos\alpha_{i-1} & -d_i * cos\alpha \\ 0 & 0 & 0 & 1 \end{bmatrix} \quad (1)$$

Then the homogeneous transformation matrix T_3^0 from the base frame to the fingertip can be obtained by the chain rule

$$T_3^0 = T_1^0 T_2^1 T_3^2 = \begin{bmatrix} C_{12} & -S_{12} & 0 & L_0 * C_1 + L1 * C_{12} \\ S_{12} & C_{12} & 0 & L_0 * S1 + L1 * S_{12} \\ 0 & 0 & 1 & 0 \\ 0 & 0 & 0 & 1 \end{bmatrix} \quad (2)$$

where C

$$C_{12} = cos(\theta_1 + \theta_2) = \cos\varphi, S_{12} = sin(\theta_1 + \theta_2) = \sin\varphi \quad (3)$$

Thus the position of the fingertip is

$$X_E = L_0 * C_1 + L_1 * C_{12} \quad (4)$$

$$Y_E = L_0 * S_1 + L_1 * S_{12} \quad (5)$$

3.2. Inverse kinematic formulation

From Section 3.1, the inverse kinematics can determine the joint movements to form a desired Cartesian position of the end-effector [36]. The solution of inverse kinematics is the key to controlling the end effector trajectories. Using Eqs. (3) and (4) and after several algebraic calculations, the inverse kinematics of the robot arm is

$$C_2 = \frac{X_E^2 + Y_E^2 - L_0^2 - L_1^2}{2L_0L_1} \quad (6)$$

and then $\theta_2$would be

$$\theta_2 = Acos(\frac{X_E^2 + Y_E^2 - L_0^2 - L_1^2}{2L_0L_1}) \quad (7)$$

To get θ_1, expressions between angles γ and θ_1, θ_2 are as

$$\theta_1 = \gamma - \beta \quad (8)$$

where

$$\gamma = Atan2(Y_E, X_E), \beta = Acos(\frac{X_E^2 + Y_E^2 + L_0^2 - L_1^2}{2L_0\sqrt{X_E^2 + Y_E^2}}) \quad (9)$$

Here, the "elbow-down" solution was chosen where the angle $\theta_2 > 0$.

The following section presents a comprehensive comparative analysis, examining the simulated results in relation to the hardware implementation.

4. Comparison and result

This section presents a detailed analysis and comparison of simulated outcomes and hardware implementation, offering insights into the performance and effectiveness of the proposed approach.

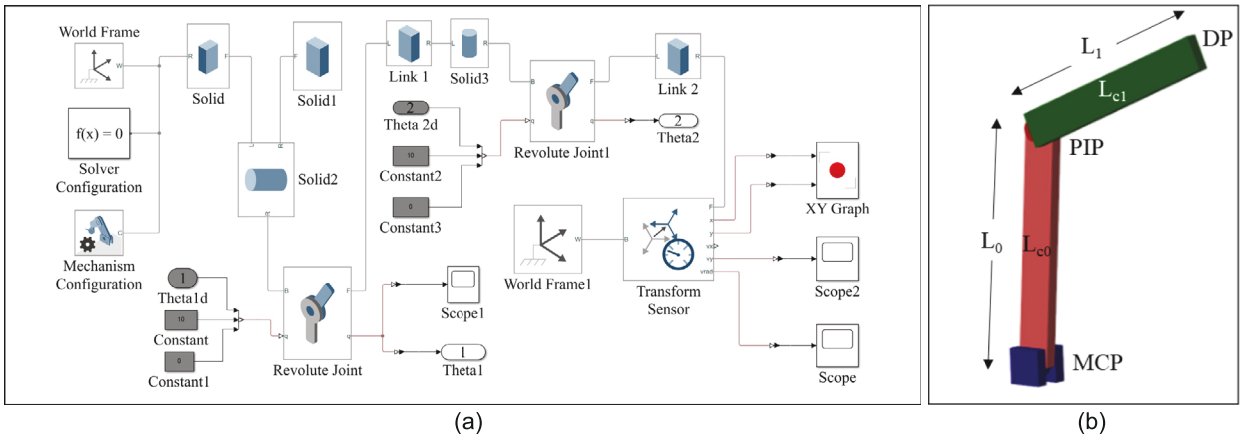

Fig. 8. Simulink simulation model of a two-link *RR* arm (a) Simulink Model description (b) 3D Model of the finger designed to mimic the aye-ayes middle finger (link).

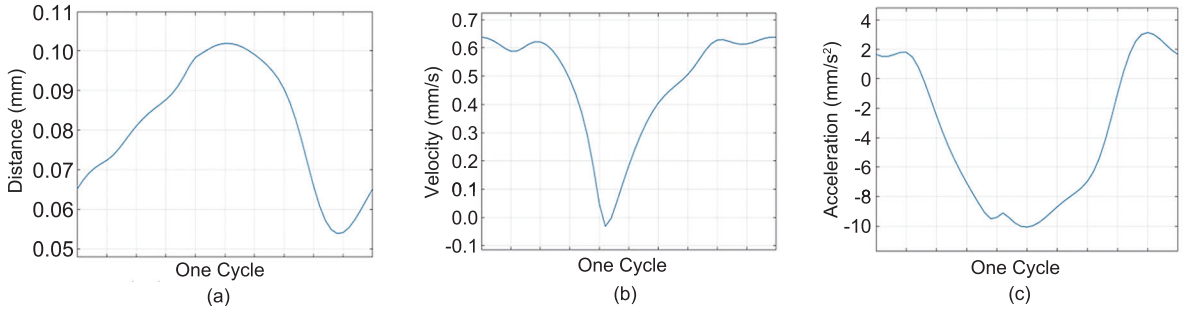

Fig. 9. Variation of (a) displacement (b) velocity, and (c) acceleration of aye-aye middle-finger tip (DP Joint) simulation.

4.1. Simulation

To simulate the derived two-link arm, a Simulink model was created with the intention of replicating the motion of aye-aye's middle finger, as seen in Fig. 8(a). A structure was designed similar to the aye-aye finger, as seen in Fig. 8(b), which was imported into this simulation.

In this experiment, the following parameters were used:

$$M_0 = 0.005 \text{ kg}, L_0 = 0.07 \text{ m}, L_{c_0} = 0.035 \text{ m}, M_1 = 0.005 \text{ kg},$$
$$L_1 = 0.04 \text{ m}, L_{c_1} = 0.02 \text{ m} \quad (10)$$

where M is the mass of the link, L is the length of the link, and L_c is the link center.

From Section 3, it was concluded that the fingertip follows a straight-line path toward the object. Thus, the initial position can be set as $X_E = 0.03$ m, $Y_E = 0.12$ m, and the final positions as $X_E = 0.1$ m, $Y_E = 0.1$ m. The initial or final angle velocities and accelerations are assumed to be zero. The variation of aye-aye middle-finger tip DP joint is shown in Fig. 9.

It can be observed that the fingertip velocity experiences an increase from half of one cycle to the end, which means the finger gets accelerated, and finally reaches its maximum speed of 0.6 m/s (see Fig. 9(b)). Compared to Fig. 7, one can notice although the scale of the speed or acceleration is larger than the real tracking values, the simulation model shares a similar pattern to the real aye-aye movement. This suggests that the *RR* link model effectively simplifies the motion of the aye-aye's finger.

4.2. Hardware implementation

To create a comprehensive hardware model, a replica of the middle finger was designed using SolidWorks. This design was based on the data gathered from motion capture tests, Simulink model simulations, and the CT scan of the bone structure of the aye-aye. This finger consists of two links, connecting the three joints MCP, PIP, and DP, offering two degrees of freedom (θ_1, θ_2). To test the overall motion of this replica finger, a hardware model was built with two standard high-speed servo motors, which were connected to the designed replica finger with the help of synthetic nylon strings. For actuation, two goBILDA 2000 Series servo motors were used, as seen in Fig. 10(b). These servos were chosen for their high speed (approx. 0.035 s/60°) and range of motion (300°) with a precise control (approx. 0.15°/μs). During the first testing phase, it was found that this finger followed a similar trajectory trend as aye-aye's middle finger but lacked structural stability, which made it difficult to test this replica tapping on a piece of wood. To strengthen the structure and improve the stability of this tapping finger, a few modifications were made to the control system and the mounting solution for the links.

To mimic the aye-aye's finger tapping, a simplistic open-loop controller was built with the help of an Arduino Microcontroller and an Adafruit 16-Channel 12-bit Servo Driver. Based on the Simulink model, appropriate parameters for the PWM signals were chosen, which provided a full range of permissible motion of both links of the finger. The overall connection block diagram of this controller can be seen in Fig. 10(a). These nylon strings served as tendons, allowing the actuation of the individual joints and resulting in a compliant finger design that closely resembles aye-aye's finger.

To simulate this and verify, the following parameters were used on Simulink:

$$M_0 = 0.02 \text{ kg}, L_0 = 0.1 \text{ m}, L_{c_0} = 0.035 \text{ m}, M_1 = 0.01 \text{ kg},$$
$$L_1 = 0.04 \text{ m}, L_{c_1} = 0.02 \text{ m} \quad (11)$$

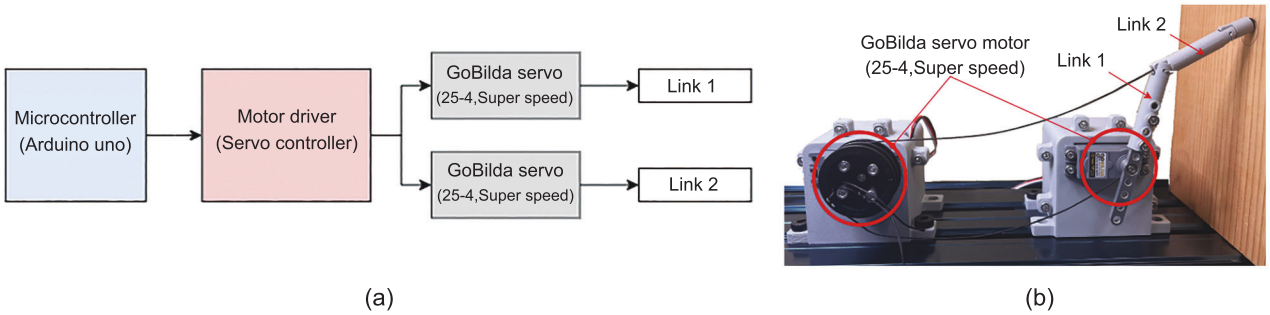

Fig. 10. The hardware model depicting the finger tapping of an aye-aye (a) Block diagram of the hardware controller used to control the actuation of the finger (b) Assembled finger incorporating tendons and motors for actuation. (The video is available at this link).

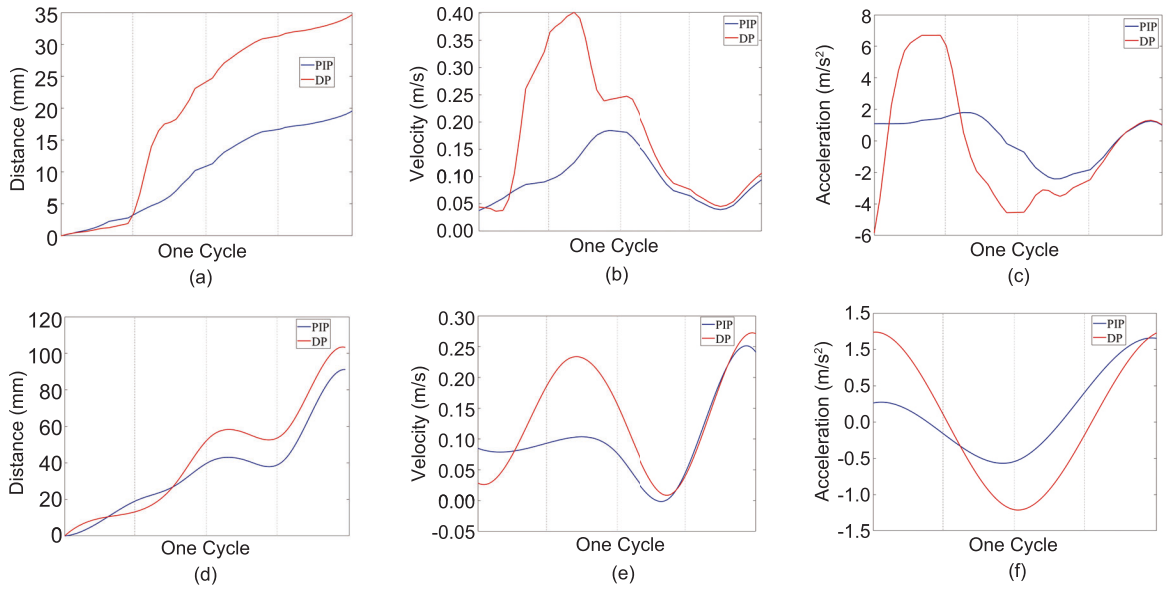

Fig. 11. Performance comparison between the hardware simulation of the finger replica (a, b, c) and the Kinovea results obtained from tracking the aye-aye's middle finger (d, e, f) in terms of variations in distance, velocity, and acceleration.

The variation of the aye-aye's middle-finger tip DP and joint PIP is depicted in Fig. 11 for the proposed hardware modeling. It is evident from the plot that the velocity of the fingertip increases at the outset of the first quarter and reaches a maximum of 0.4 m/s in the middle of the second quarter, indicating a high acceleration of the finger during this period. Based on the results obtained from the Kinovea Motion Tracking software, the overall variation in the aye-aye's middle finger with respect to the distance, velocity, and acceleration can be seen in Fig. 11(d) to (f). The DP Joint and the PIP Joints of the finger seem to follow a similar deflection as seen in Fig. 11(a). As observed in Fig. 11(e), at the beginning of the cycle, the fingertip makes contact with the object at a minimum speed of 0.05 m/s and reaches its maximum speed of 0.25 m/s. Compared to Fig. 11(b), one can see that the maximum speed of the DP joint is larger than the actual tracking value because the mimicking model is heavier than the real aye-aye finger, and the length is also significantly bigger than that of the real one. The mimicking acceleration is also shown in Fig. 11(c), with a bigger scale than the real tracking value for the same reason. But the mimicking model also shares a similar pattern to aye-aye's finger-tapping motion.

Upon comparing the performance parameters obtained from the hardware model as well as the Kinovea, as seen in Fig. 11, it was observed that the hardware model followed a similar trajectory as the aye-aye's middle finger based on the motion tracking results obtained but was not able to match the speed at which it was the finger was tapping on the surface. It was also observed that the maximum reach of the finger was significantly higher than what the aye-aye would have achieved since the motor and tendons joint proved inefficient in providing precise link control. An overall comparison between the aye-aye tapping, the proposed Simulink model, and the proposed hardware model can be seen at this link.

5. Conclusions

This study pursues three primary objectives. Firstly, it utilizes a motion-tracking technique to analyze the intricate movements of the aye-aye's middle finger by examining videos of the animal. Secondly, a simplified two-link robot arm model is constructed to replicate the observed finger trajectory effectively. Lastly, a hardware model is developed to accurately simulate the intricate movements of the aye-aye's finger.

The model was derived by tracking the MCP, PIP, and DP joints captured from a video. A dynamic *RR* robot model was constructed to replicate the tapping motion of the finger. Although the data obtained from the hardware implementation is slightly higher at the DP joint (approx. 0.4 m/s) than the Simulink Simulation results (approx. 0.6 m/s) of the modeled finger, the preliminary results from this study seem to follow a similar

trajectory when compared to the video of the aye-aye tapping on the wooden bark.

A more accurate investigation should be further studied because of the complexity of the aye-aye's middle finger kinematics. The current mimicking model is more significant than the real one, which causes a big scale in speed and acceleration. Kinovea emerges as a trustworthy and freely available software that generates valid data. By digitizing x- and *y*-axis coordinates and placing markers on individual joints, it provides an acceptable level of accuracy when measuring angular and linear dimensions. However, the authors express their intention further to investigate the motion trajectories of the animal's finger using an improved camera and alternative tracking methodologies to reduce error further and enhance accuracy. To address this, future endeavors should focus on constructing more precise hardware that closely matches the aye-aye's actual finger. Moreover, enhancements to the dynamic model are imperative to accommodate diverse trajectory planning requirements.

Declaration of competing interest

The authors declare that they have no known competing financial interests or personal relationships that could have appeared to influence the work reported in this paper.

Acknowledgments

The authors would like to thank the US National Science Foundation (NSF) for their financial support. This research effort was funded under NSF CAREER Award Number 2047033. This work was performed in part at the Duke University Shared Materials Instrumentation Facility (SMIF), a member of the North Carolina Research Triangle Nanotechnology Network (RTNN), which is supported by the National Science Foundation, United States (ECCS-1542015) as part of the National Nanotechnology Coordinated Infrastructure (NNCI). The authors express their sincere appreciation for the invaluable assistance of Dr. Erin Ehmke from Duke Lemur Center (DLC). Additionally, the authors extend their gratitude to David Haring from DLC for supplying a photo of the aye-aye during tap-scanning.

References

[1] C.J. Erickson, S. Nowicki, L. Dollar, N. Goehring, Percussive foraging: Stimuli for prey location by aye-ayes (*Daubentonia madagascariensis*), Int. J. Primatol. 19 (1) (1998) 111–122.
[2] J. Petter, R. Albignac, Y. Rumpler, Faunes de Madagascar, vol. 44, Mammifères lémuriens (primates prosimiens). Paris: Orstom, 1977.
[3] E.J. Sterling, E.E. McCreless, Adaptations in the aye-aye: A review, Lemurs (2006) 159–184.
[4] C.J. Erickson, Percussive foraging in the aye-aye, *Daubentonia madagascariensis*, Anim. Behav. 41 (5) (1991) 793–801.
[5] M.A. Ramsier, N.J. Dominy, Receiver bias and the acoustic ecology of aye-ayes (*Daubentonia madagascariensis*), Commun. Integr. Biol. 5 (6) (2012) 637–640.
[6] G.H. Perry, D. Reeves, P. Melsted, A. Ratan, W. Miller, K. Michelini, E.E. Louis Jr., J.K. Pritchard, C.E. Mason, Y. Gilad, A genome sequence resource for the aye-aye (*Daubentonia madagascariensis*), a nocturnal lemur from Madagascar, Genome Biol. Evol. 4 (2) (2012) 126–135.
[7] C. Schwitzer, R.A. Mittermeier, A.B. Rylands, F. Chiozza, E.A. Williamson, J. Wallis, A. Cotton, Primates in peril, 2015, The World's 25 Most Endagered Primates 2014-2016.
[8] A.T. Feistner, E.J. Sterling, Body mass and sexual dimorphism in the aye-aye *Daubentonia madagascariensis*, Dodo 31 (1995) 73–76.
[9] K.E. Glander, Morphometrics and growth in captive aye-ayes (*Daubentonia madagascariensis*), Folia Primatol. 62 (1–3) (1994) 108–114.
[10] A.H. Schultz, The skeleton of the Hylobatidae and other observations on their morphology, Gibbon Siamang 2 (1973) 1–54.
[11] H. Nemati, E. Dehghan-Niri, The acoustic near-field measurement of aye-ayes' biological auditory system utilizing a biomimetic robotic tap-scanning, Bioinspiration Biomim. 15 (5) (2020) 056003.
[12] J.-J. Petter, The aye-aye, Primate Conservation (1977) 37–57.
[13] E.J. Sterling, Aye-ayes: Specialists on structurally defended resources, Folia Primatol. 62 (1–3) (1994) 142–154.
[14] T. Iwano, C. Iwakawa, Feeding behaviour of the aye-aye (*Daubentonia madagascariensis*) on nuts of ramy (*Canarium madagascariensis*), Folia Primatol. 50 (1–2) (1988) 136–142.
[15] T.M. Sefczek, Z.J. Farris, P.C. Wright, Aye-aye (*Daubentonia madagascariensis*) feeding strategies at Ranomafana National Park, Madagascar: An indirect sampling method, Folia Primatol. 83 (1) (2012) 1–10.
[16] C. Soligo, Anatomy of the hand and arm in *Daubentonia madagascariensis*: A functional and phylogenetic outlook, Folia Primatol. 76 (5) (2005) 262–300.
[17] G.W. Milliken, J.P. Ward, C.J. Erickson, Independent digit control in foraging by the aye-aye (*Daubentonia madagascariensis*), Folia Primatol. 56 (1991) 219–224.
[18] S. Lhota, T. Junek, L. Bartos, Patterns and laterality of hand use in free-ranging aye-ayes (*Daubentonia madagascariensis*) and a comparison with captive studies, J. Ethol. 27 (3) (2009) 419–428.
[19] S. Lhota, T. Junek, L. Bartos, A.A. Kubena, Specialized use of two fingers in free-ranging aye-ayes (*Daubentonia madagascariensis*), Am. J. Primatol.: Official J. Am. Soc. Primatologists 70 (8) (2008) 786–795.
[20] R. Owen, Monograph on the Aye-Aye (Chiromys Madagascariensis, Cuvier), Taylor & Francis, 1863.
[21] T.L. Kivell, D. Schmitt, R.E. Wunderlich, Hand and foot pressures in the aye-aye (*Daubentonia madagascariensis*) reveal novel biomechanical trade-offs required for walking on gracile digits, J. Exp. Biol. 213 (9) (2010) 1549–1557.
[22] R.M. Winn, Development of behaviour in a young aye-aye (*Daubentonia madagascariensis*) in captivity, Folia Primatol. 62 (1–3) (1994) 93–107.
[23] E. Krakauer, P. Lemelin, D. Schmitt, Hand and body position during locomotor behavior in the aye-aye (*Daubentonia madagascariensis*), Am. J. Primatol.: Official J. Am. Soc. Primatologists 57 (3) (2002) 105–118.
[24] C.E. Oxnard, The uniqueness of Daubentonia, Am. J. Phys. Anthropol. 54 (1) (1981) 1–21.
[25] A.T. Feistner, E.C. Price, G.W. Milliken, Preliminary observations on hand preference for tapping, digit-feeding and food-holding in captive aye-ayes (*Daubentonia madagascariensis*), Folia Primatol. 62 (1–3) (1994) 136–141.
[26] Q. Xu, C. Cai, H. Zhou, H. Ren, A video tracking system for limb motion measurement in small animals, in: 2010 International Conference on Optoelectronics and Image Processing, Vol. 1, IEEE, 2010, pp. 181–184.
[27] A. Weisenberger, S. Gleason, J. Goddard, B. Kross, S. Majewski, S. Meikle, M. Paulus, M. Pomper, V. Popov, M. Smith, et al., A restraint-free small animal SPECT imaging system with motion tracking, IEEE Trans. Nucl. Sci. 52 (3) (2005) 638–644.
[28] P. Perner, Motion tracking of animals for behavior analysis, in: International Workshop on Visual Form, Springer, 2001, pp. 779–786.
[29] X. Zhang, C. Zhao, Z. Xu, S. Huang, Mechanism analysis of cheetah's high-speed locomotion based on digital reconstruction, Biomimetic Intell. Robot. 2 (1) (2022) 100033.
[30] D. Murray, A. Basu, Motion tracking with an active camera, IEEE Trans. Pattern Anal. Mach. Intell. 16 (5) (1994) 449–459.
[31] A. Koehnsen, J. Kambach, S. Büsse, Step by step and frame by frame–workflow for efficient motion tracking of high-speed movements in animals, Zoology 141 (2020) 125800.
[32] kinovea, www.kinovea.org, 2020, www.kinovea.org/.
[33] A. Puig-Diví, C. Escalona-Marfil, J.M. Padullés-Riu, A. Busquets, X. Padullés-Chando, D. Marcos-Ruiz, Validity and reliability of the kinovea program in obtaining angles and distances using coordinates in 4 perspectives, PLoS One 14 (6) (2019) e0216448.
[34] N. Shishov, K. Elabd, V. Komisar, H. Chong, S.N. Robinovitch, Accuracy of kinovea software in estimating body segment movements during falls captured on standard video: Effects of fall direction, camera perspective and video calibration technique, PLoS One 16 (2021) 1–22.
[35] P. Braido, X. Zhang, Quantitative analysis of finger motion coordination in hand manipulative and gestic acts, Hum. Mov. Sci. (ISSN: 0167-9457) 22 (6) (2004) 661–678.
[36] R. Jazar, Theory of Applied Robotics: Kinematics, Dynamics and Control and Control, Springer, 2010.